A R C H I V E S   O F   M E T A L L U R G Y   A N D   M A T E R I A L S

Volume 50 2005 Issue 2

W. RATUSZEK*, J. KOWALSKA*, J. AUGUSTYN-PIENIĄŻEK*, K. CHRUŚCIEL*

DEFORMATION AND RECRYSTALLIZATION TEXTURES IN SINGLE PHASE Ag-Cd ALLOYS

TEKSTURY ODKSZTAŁCENIA I REKRYSTALIZACJI W JEDNOFAZOWYCH STOPACH Ag-Cd

Deformation and recrystallization textures were examined in pure Ag and Ag with 10, 15, 20 and 30 wt.% Cd additions. The materials were cold-rolled up to 90% of deformation and subsequently annealed within the range of temperatures 170-310°C for 20, 60 and 120 min in dependence on the chemical composition. The influence of alloy addition on the texture development was investigated due to the fact that the electron density coefficient increases, while the stacking fault energy (SFE) decreases with the increasing content of Cd.

The texture after deformation could be described by a limited α fibre <110> ND with main component {110}<225> and a weak γ fibre {111}<uvw>. After annealing the α fibre became weak and extended, the maximum of the orientation distribution function (ODF) value shifted towards the {110<110> orientation and the γ fibre decayed. New components appeared: a limited {113}<uvw> fibre and {430}<340>, {412}<548>, {523}<638> orientations. Although the cadmium addition did not affect much the deformation texture, its influence on recrystallization texture was more pronounced.

The relationship between deformation and annealing textures was described by the 35-40° rotation around <111> poles, for oriented growth or by the rotation about the (2n-1) × 60° angle around <111> poles, for twinning. The orientations formed during further annealing can be described by the 22-30° rotation angle around <111> poles of the previous textures.

Small volume of twinned areas was observed in the microstructure after large deformation. The formation of twins during annealing and their selective growth indicated that they played an important role in the recrystallization process.

Przedmiot badań stanowiło srebro i jego stopy Ag-Cd (10, 15, 20 i 30% masowych Cd). Materiał walcowano na zimno do 90% odkształcenia i następnie wyżarzano w zakresie temperatur 170-310°C (w zależności od składu chemicznego) przez czas 20, 60 i 120 minut. Badano wpływ dodatku stopowego na rozwój tekstury, wraz ze wzrostem zawartości kadmu wzrasta stężenie elektronów (e/a) natomiast energia błędu ułożenia (EBU) maleje.

Teksturę po odkształceniu opisuje ograniczone włókno α (<110>|| KW) z główną składową {110}<225> i słabe włókno γ {111}<uvw>. W wyniku wyżarzania włókno

* WYDZIAŁ METALURGII I INŻYNIERII MATERIAŁOWEJ, AKADEMIA GÓRNICZO-HUTNICZA, 30-059 KRAKÓW, AL. MICKIEWICZA 30

α ulega osłabieniu i rozciągnięciu, maksimum orientacji przesuwa się w kierunku orientacji {110}<110>, zanika włókno γ, pojawiają się nowe składowe np. ograniczone włókno {113}< uvw> i orientacje {430}<340>, {412}<548>, {523}<638>. Dodatek stopowy Cd nie wpłynął istotnie na teksturę odkształcenia, natomiast wyraźniejszy był wpływ kadmu w przypadku tekstury rekrystalizacji.

Relacje pomiędzy orientacjami występującymi w teksturze odkształcenia a orientacjami tekstury rekrystalizacji można opisać obrotem o kąt około 40° wokół biegunów <111> i obrotem (2n-1) × 60° wokół biegunów <111>- relacją bliźniaczą, zaś orientacje powstałe w dalszym etapie wyżarzania obrotami o kąty 22- 30° wokół biegunów <111> uprzednio powstałych orientacji.

W mikrostrukturze po dużych stopniach odkształcenia obserwuje się niewielką ilość obszarów zbliźniaczonych na tle pasm ścinania. Tworzenie się bliźniaków w czasie wyżarzania a następnie selektywny wzrost wskazują na ich istotną rolę w procesie rekrystalizacji.

1. Introduction

The stacking fault energy SFE is a most popular parameter to describe properties of metals and alloys. The differences between deformation and annealing textures of FCC metals can be explained by changes of SFE. The electron density coefficient (e/a) is another factor useful in the analysis of the correlation between SFE and the properties of FCC metals. When this concentration increases, the SFE of solid solutions lowers, while the probability of appearance of stacking faults (α) grows [1]. The difference of valences between the solvent and the solute element as well as size parameter S_F defined as S_F = [R(solute)- R(solvent)]/R(solvent), where R is a radius of atom) is very important [2]. The mutual solubility of two elements depends on their valences in such a way, that the solubility of element with lower valence is larger. It refers to Cu and Ag alloys [3, 4]. M. De and coworkers [2] and Delehouzee and coworkers [5] investigated the influence of alloy additions on the probability of stacking fault appearance and, in consequence on the SFE value in a numbers of alloys [2, 5].

The metals and alloys can be divided into groups of low, medium and high SFE. Silver and its alloys belong to the first group of metals with low SFE. With the aim to explain the deformation and recrystallization texture, the investigations on polycrystals [6-8] and monocrystals [9-11] were performed. The formation of texture also depends on many parameters such as: initial orientation, chemical composition, conditions of plastic working, conditions of annealing and grain size [12, 13].

Two theories explaining the mechanisms of recrystallization texture formation were proposed: orientation nucleation theory and oriented growth theory [14, 15]. Twinning is also very important for the texture development in FCC materials with low SFE [16, 17].

The aim of this work was to analyze the annealing texture at different contents of cadmium in dependence on temperature and annealing time as well as some global aspects of recrystallization texture formation and its development in silver alloys.

2. Materials and experimental procedure

The object of investigations was Ag and Ag alloys with different contents of cadmium (up to 30 wt.%). The cast material was deformed up to 50% and then polished to dimensions 15 × 300 × 100 mm and annealed in vacuum at temperature $T_{anneal} = 2/3T_{melt}$ adequate for each alloy. The prepared materials were cold rolled up to 90% and annealed according to the same formula (table 1).

TABLE

Chemical composition, conditions of annealing, ideal orientation and the maximum values of the ODF's for Ag and AgCd alloys

Materials	% Cd wt.% at.%	Value e/a	Conditions of annealing		Orientation {hkl} <uvw>	Max F(g)
			Temp. [°C]	Time [h]		
			—	—	{011}<225>	12
Ag	—	—	310	1	{011}<011>	4.6
			310	2	{034}<043>	2.7
	10		—	—	{011}<225>	8.1
AgCd10		1.096	310	1	~{123}<385>	3.2
	9.638		310	2	~{113}<121>	3.0
	15		—	—	{011}<113>	9.6
AgCd15		1.144	310	1	~{113}<121>	2.9
	14.486		310	2	~{113}<121>	2.9
	20		—	—	{011}<113>	9.2
AgCd20		1.193	290	1	~{113}<121>	2.9
	19.354		290	2	~ {113}<121>	3.8
	30		—	—	{011}<225>	7.6
AgCd30		1.291	270	1	~{113}<121>	3.5
	29.149		270	2	~{113}<121>	3.3

Metallographic examinations were conducted by means of Zeiss optical microscope Axiovert 200 MAT. Electrolytic etching was applied to reveal the microstructure. The investigations were carried out on longitudinal sections (on the plane perpendicular to the transverse direction) using transmission electron microscopy JEOL JEM 200 CX. Thin foils were produced of longitudinal sections (ND-RD).

X-ray texture measurements were conducted by means of Bruker diffractometer D8 Advance using $Co_{K\alpha}$ radiation ($\lambda_{K\alpha} = 1,79Å$). Texture measurements were carried out by means of the back-reflection method from the centre layer of the sheet. Using three incomplete pole figures of planes: {111}, {200} and {311} the ODF's were calculated. Transformation of deformation textures to recrystallization textures was performed (Fig. 5-9).

3. Analysis of experimental results

The microstructure of the material after deformation and annealing is showed in Figs. 1-4. It is typical for materials with low SFE. The waved microbands localized

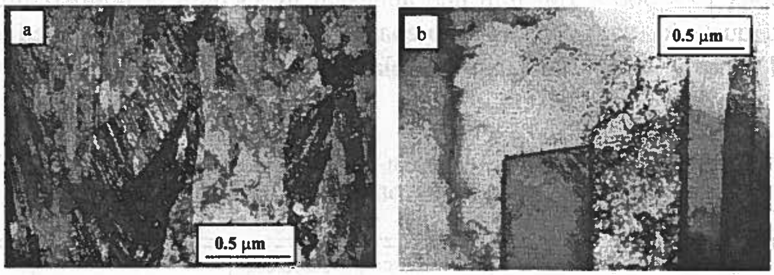

Fig. 1. Microstructure of the Ag after 90% of deformation (a) and recrystallization at 310°C/1hour (b); on the longitudinal section ND-RD of the sheet, TEM

parallel to the rolling plane and lenticular areas dispersed in microbands are presented in Fig. 2a, 3a. The lamellar structure containing deformation twins can be visible in the images. The twins rotated and its longer axes had direction almost parallel to the rolling direction (Fig. 1a, 3b).

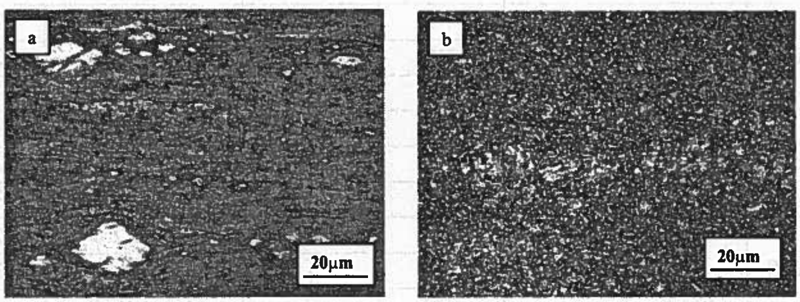

Fig. 2. Microstructure of the Ag Cd 15 alloy after 90% of deformation (a) and recrystallization at 290°C/2hours (b); on the longitudinal section Nd-RD of the sheet, optical microscopy

In the annealed material the equiaxial grains of different size were observed, which indicated that grain growth occurred during heating (Fig. 2b, 4a). The electron microscopy observations revealed many recrystallization twins, whose density depended on chemical composition, temperature and time of annealing (Fig. 1b, 4b).

The texture of silver after 90% deformation is described by the limited α fibre <110>|| ND with main component {110}<225>, very weak {111}<112> orientations and weak and spread {637}<195> orientations (Fig. 5a, 6, 7).

After an hour annealing at 210°C, the extent of α-fibre and shift of maximum FRO value toward {110}< 110 > orientation took place. G o s s {110}< 001 > and

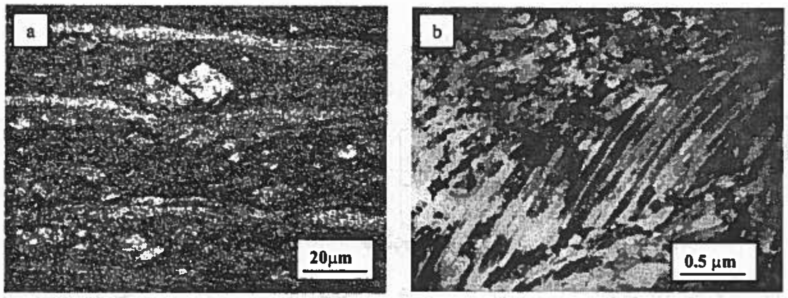

Fig. 3. Microstructure of the Ag Cd 30 alloy after 90% deformation, optical microscopy (a) TEM (b); on the longitudinal section ND-RD of the sheet

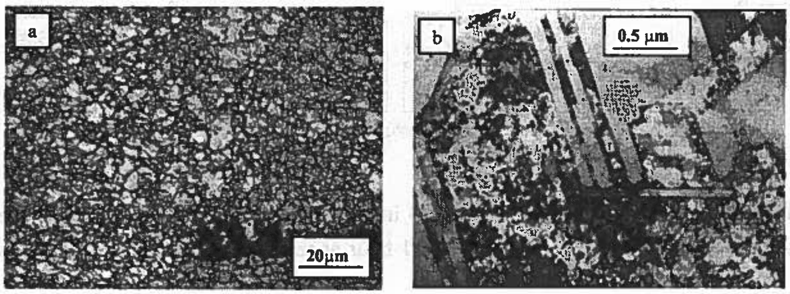

Fig. 4. Microstructure of the Ag Cd 30 alloy after 90% of deformation and recrystallization at 270°C/2 hours, optical microscopy (a), TEM (b); on the longitudinal section ND-RD of the sheet

Bs {110}<112> orientation intensities decreased. The γ- fibre <111>|| ND became quite weak. Meanwhile, new orientations such as {113}<332> with streaks towards {114}<221> and {112}<111> appeared. Additionally, weak orientations {215}<211>, {214}<845>, {523}<638>, {263}<358> and cubic orientation {100}<001> were al so recorded.

The annealing at 310°C for 1 hour brought about small changes in the recrystallization texture. The α fibre spread towards the {058}<085> orientation, also the Goss component {110}<001> weakened, while the {110}<112> and {100}<001> orientations completely decayed (Fig. 5b, 6-8).

The further annealing, up to 2 hours, led to the disappearance of the orientation {110}<001> and {110}<112> from the α fibre. Moreover, the α fibre was partially separated and maximum ODF value shifted from the {110}<110> to {034}<043> orientation. There was no cubic orientation any longer. The spread {113}<332> and {215}<320> orientations remained weak and almost did not change (Fig. 5c, 7, 8).

The Ag Cd 10 alloy after 90% deformation contained a limited α fibre with main component {110}<225> and weak γ-fibre <111>|| ND (Fig. 6, 7). After an hour annealing at 210°C, the decrease of intensity of main components in the deformation texture was observed. The maximum ODF value shifted towards the {110}<113>

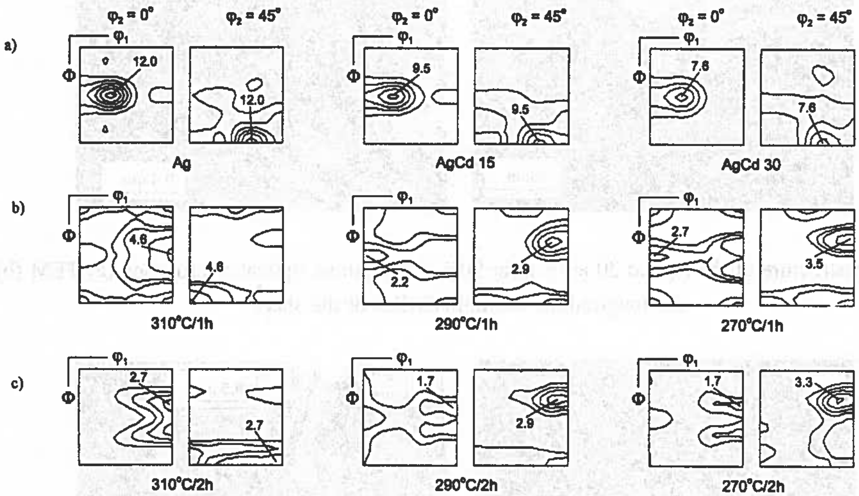

Fig. 5. Orientation distribution functions (ODF's) in sections $\varphi_2 = 0°$, $\varphi_2 = 45°$ for the pure Ag and Ag-Cd alloys after 90% deformation (a); after 1 hour annealing (b); after 2 hour annealing (c)

orientation, the γ-fibre decayed whereas very weak orientations such as {113}<332>, {215}<211>, {214}<845>, {523}<638>, {100}<001> appeared.

After annealing at 310°C for 1 hour, the maximum ODF value shifted towards {034}<043> orientation and the α fibre extended to the {110}<110> one. The Goss orientation was found to be weak contrary to the {113}<332>, {215}<211>, {214}< 845>, {523}<638 > orientations. The small increase of intensity of cubic orientation {100}<001> was observed (Fig. 6-8).

2 hour-annealing led to the separation of the α fibre in its end part and a further decrease of the intensity of G o s s orientation. The cubic orientation completely disappeared.

The Ag Cd 15 and Ag Cd 20 alloys acquired a fibre texture after the deformation containing the limited α fibre <110>|| ND with {110}<113> as main component and the weak γ-fibre <111>|| ND (Fig 5a, 6, 7). After annealing at 190°C for 1 hour the texture intensity increased indicating that recovery process had begun. An early stage of recrystallization was also observed by extending the α fibre. The γ-fibre still existed in the texture.

When the annealing temperature was increased to 290°C the orientations of the α fibre weakened and the γ-fibre decayed, while the limited {113}<uvw> fibre appeared blurred. The orientations {215}<211>, {214}<845>, {523}<638> were stronger than other orientations. Weak cubic orientation was found in the texture (Fig. 5b, 6-8). 2

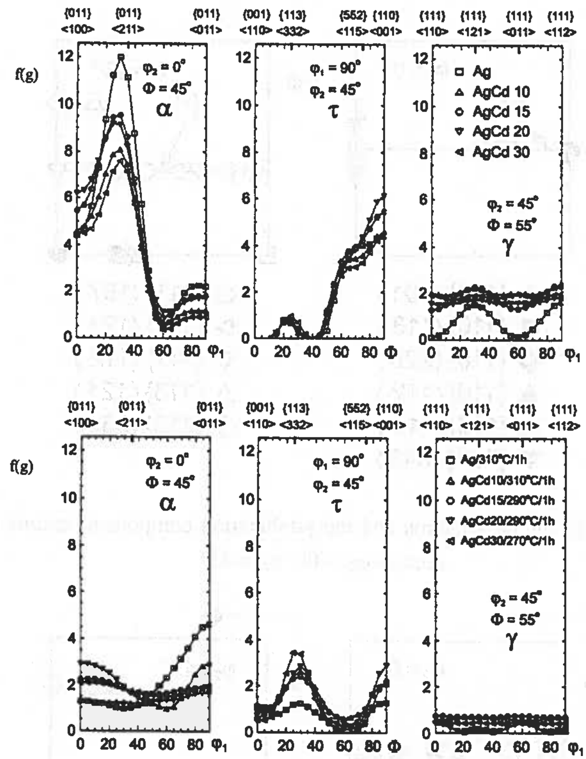

Fig. 6. Values of orientation distribution function f(g) along the fibres α, τ and γ for 90% of deformation and recrystallization of pure Ag and Ag-Cd alloys

hour annealing of the Ag Cd 15 alloy effected in the decay of main components of deformation texture and the appearance of a limited {034}<uvw> fibre and a strong {113}<uvw> one (Fig. 5c, 6-8). In the Ag Cd 20 alloy a complete decay of the α fibre and a separation towards {059}<095> orientation took place. A strong {113}<332−574> fibre and a weak {059}<100> orientation were observed, while the Goss orientation disappeared.

In the Ag Cd 30 alloy after 90% of deformation, one can observe the limited α fibre with main component {110}<225> and the weak homogenous γ-fibre (Fig. 5a, 6, 7). Annealing at 170°C for 1 hour led to the beginning of the recovery process judging from the increase of texture intensity. The α fibre extended and the intensity of the Goss orientation increased. The orientations typical for the γ-fibre were also observed in the texture.

Annealing at 270°C for the same time led to weakening of the intensity of deformation texture components. The α fibre separated into two parts. The limited {113}<uvw> fibre contained the {113}<211> orientation as the strongest component. One can also observe strong texture components {215}< 211 >, {523}< 638 >, {326}< 385 > as

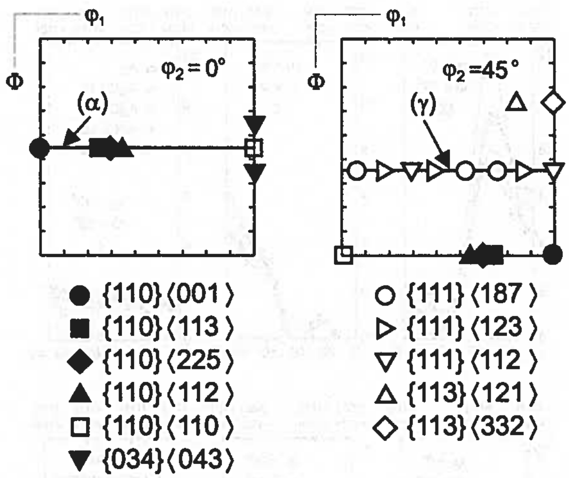

Fig. 7. Major position of the deformation and recrystallization components texture on the ODF's on section $\varphi_2 = 0°$, $\varphi_2 = 45°$

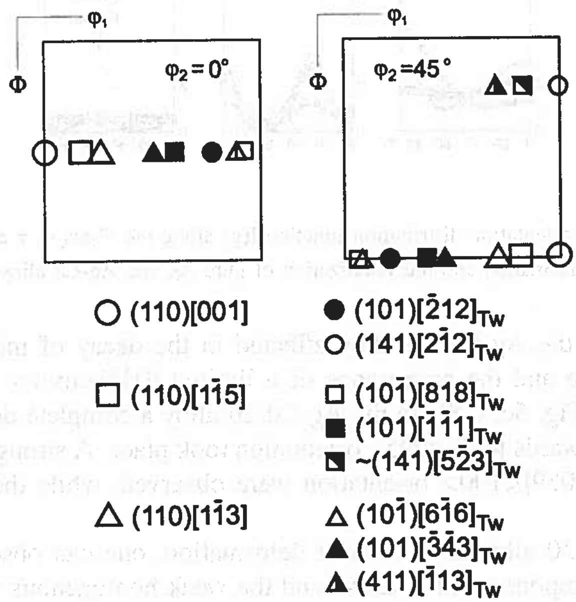

Fig. 8. Transformation of the ideal orientations {110}<*uvw*> α-fibre from the rolling texture to the recrystallizations texture according to twin relations (2n-1)×60°, section $\varphi_2 = 0°$, $\varphi_2 = 45°$

well as a weak cubic one (Fig. 5b, 6-8). Annealing for 2 hours led to the decay of the α fibre, while the weak Goss orientation remained. The {113}<112> orientation became the strongest. Simultaneously, the {113}< uvw > fibre underwent spreading. The {214}<845>, {523}<638> orientations were found to be also strong. The typical

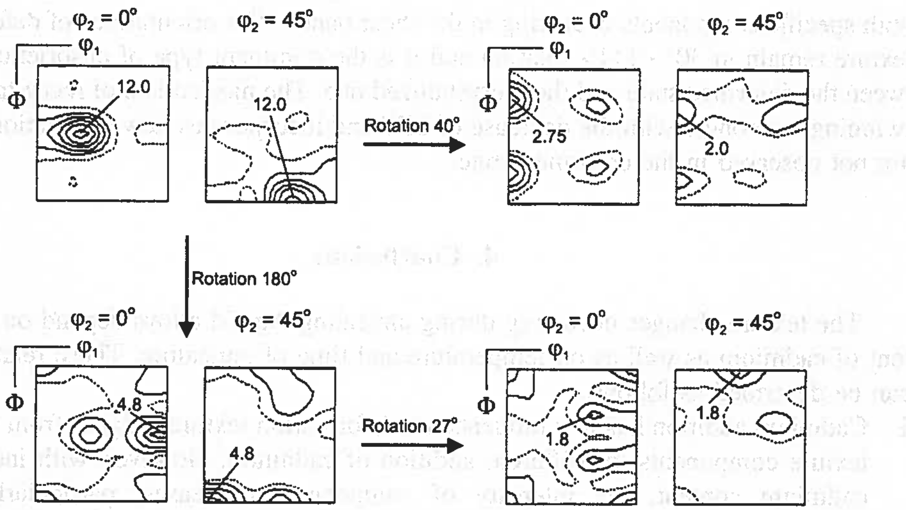

Fig. 9. Transformation of the experimental ODF's by rotations about 40, 180 and 27° angles around <111> poles, section $\varphi_2 = 0°$, $\varphi_2 = 45°$

{263}<385> orientation of the recrystallization texture was identified as well (Fig. 5c, 7, 8).

In order to analyze better the crystallographic relationships between deformation and annealing texture of Ag, the transformation of experimental ODF's was performed by the rotation about specified angles (Fig. 9). The transformation of single orientations of deformation texture, which indicate that recrystallization texture can be obtained by the rotation by angle 35-40° and 22-27° around the <111> poles and for the twin relation by the angle (2n-1) × 60° was performed. However, the selective choice of the rotation axes should be taken into account. The orientations of deformation texture from the α fibre <110>|| ND formed a twin relation with the orientations from the same fibre as well as with the {114}<uvw> ones. The orientations laying in the spread of Goss orientation {110}<001> were in twin relationship with the {113}< uvw > orientations. Other ones laying in spread of Bs orientation {110}<112> could be described by 35-40° relation with {214}<215> orientations (Fig. 7-9).

S z t w i e r t n i a [16] investigated local orientations in particular places of deformation and recrystallization microstructure. He found that during transformation one could observe two stages. The beginning stage, which strongly depends on local microstructure and can be described by an oriented nucleation and another, which refers to selective growth of nuclei in the global texture. This texture contains main orientations describing the texture typical for low SFE materials. The texture of CuZn22 alloy seems very similar to the texture of Ag alloys with larger content of cadmium.

P a u l [15] claims that recrystallization twinning may be considered as secondary mechanism. He investigated the microtexture changes at the beginning stage of recrystallization. He found that these changes might be explained by the nucleation of areas with specific components occurring in the shear bands. The orientations of deformation texture remain in 30° <111> relation and it is the dominant type of desorientation between the deformed state and the recrystallized one. The mechanism of recrystallization twinning is stronger with the decrease of SFE and incorporates new orientations which are not observed in the deformed state.

4. Conclusions

The texture changes occurring during annealing Ag-Cd alloys depend on the content of cadmium as well as on temperature and time of annealing. These relationships can be described as follows.

1. Cadmium addition has low influence on deformation texture judging from the same texture components for different addition of cadmium. However, with increase of cadmium content, the intensity of components decreases, particularly, when {110}<225> component, close to B_s{110} <112> is to be considered. Moreover, low contribution of orientations from the γ-fibre <111>|| ND was observed.
2. Annealing Ag Cd (10-30) alloys within the low range of temperatures led to the recovery process (increase of texture intensity), contrary to pure silver, which recrystallizes.
3. The annealing within higher range of temperatures (270-290°C) for 1 and 2 hours led to the spread and extension of the α fibre <110>|| ND. That fibre separated in the end part in the limited {034}< uvw > fibres.
4. The progress of recrystallization effected in the appearance of new orientations: the spread {113}<332>, {114}<221>, {215}<211>, {214}<845>, {523}<638> ones and the {263}<358> orientation, typical for the recrystallization texture of low SFE materials).
5. The relationship between the deformation and annealing textures can be described with rotation by 35-40° angle around <111> poles for oriented growth, and with he rotation by (2n-1)×60° angle around <111> poles for twinning. The newly formed orientations can be defined with the rotation by 22-30° angle around <111> poles of previous annealing textures.
6. The recrystallization proceeded by the oriented growth as well as the nucleation and the selective growth of twins.

Acknowledgements

Authors gratefully acknowledge financial support from the Polish Committee of Scientific Research (KBN) under the contract No 11.110.230.

REFERENCES

[1] P.C.J. Gallagher, Metallurgical Transactions, 1, 1970 2429.
[2] M. De, S.P. Sen Gupta, Scripta Metallurgica 26, 1373 1974.

[3] W. Hume-Rothery, Elements of Structural Metallurgy; London Inst. Metals. 1962.
[4] W. Ratuszek, Tekstury odkształcenia i wyżarzania w stopach na osnowie miedzi, Rozprawy monografie AGH, Kraków 1995.
[5] L. Delehouzee, A. Deruyttere, Acta Metallurgica **15**, 727 (1967).
[6] K. Sztwiertnia, Materials Science Forum **408-412**, 767 (2002).
[7] K. Sztwiertnia, Mechanizmy formowania się tekstur rekrystalizacji w metalach i stopach o sieci RSC, PAN, 2001, Kraków.
[8] H.J. Shin, H.T. Jeong, D.N. Lee, Materials Science and Engineering. **279A**, 244 (2000).
[9] F. Haessner, G. Hoschek, G. Tolg, Acta Metallurgica **27**, 1539 (1979) .
[10] H. Paul, J.H. Driver, C. Maurice, Z. Jasieński, Acta Materialia **50**, 4339 (2002).
[11] H. Paul, Mikroteksturowe uwarunkowania procesu rekrystalizacji pierwotnej w metalach o sieci A1, PAN , 2002, Kraków.
[12] C. Donadille, R. Valle, R. Penelle, Akta Metallurgica **37**, 305 (1989).
[13] K. Lucke, O. Engler, Materials Science and Technology **6**, 1113 (1990).
[14] P.A. Beck, Letter to the Editor, Acta Metall. **1**, 230 (1953).
[15] K. Lucke, The formation of recrystallization textures in metals and alloys ,Proc 7-th Int. Conf. on Textures of Materials, ICOTOM-7, Nordvijkerhout.
[16] S. Hoekstra, J.W.H.G. Slakhorst, J. Hubert, Acta Metallurgica **25**, 395-406 (1977).
[17] D.N. Lee, Scripta Metallurgica et Materialia **32**, 10, 1689 (1995).

Received: 21 March 2005.